Conversion of Type I 4:6 to 3:5 β-Turn Types in Human Acidic Fibroblast Growth Factor: Effects upon Structure, Stability, Folding, and Mitogenic Function

Jihun Lee,[1] **Vikash Kumar Dubey,**[2] **Thayumanasamy Somasundaram,**[3] **and Michael Blaber**[2]*

[1]*Department of Chemistry and Biochemistry, Florida State University, Tallahassee, Florida 32306-4300*
[2]*Department of Biomedical Sciences, Florida State University, Tallahassee, Florida 32306-4300*
[3]*Kasha Institute of Molecular Biophysics, Florida State University, Tallahassee, Florida 32306-4300*

ABSTRACT Human acidic fibroblast growth factor (FGF-1) is a member of the β-trefoil superfold, a protein architecture that exhibits a characteristic threefold axis of structural symmetry. FGF-1 contains 11 β-turns, the majority being type I 3:5; however, a type I 4:6 turn is also found at three symmetry-related locations. The relative uniqueness of the type I 4:6 turn in the FGF-1 structure suggests it may play a key role in the stability, folding, or function of the protein. To test this hypothesis a series of deletion mutations were constructed, the aim of which was to convert existing type I 4:6 turns at two locations into type I 3:5 turns. The results show it is possible to successfully substitute the type I 4:6 turn by a type I 3:5 turn with minimal impact upon protein stability or folding. Thus, these different turn structures, even though they differ in length, exhibit similar energetic properties. Additional sequence swapping mutations within the introduced type I 3:5 turns suggests that the turn sequence primarily affects stability but not turn structure (which appears dictated primarily by the local environment). Although the results suggest that a stable, foldable β-trefoil protein may be designed utilizing a single turn type (type I 3:5), a type I 4:6 turn at turn 1 of FGF-1 appears essential for efficient mitogenic function. Proteins 2006;62:686–697. © 2005 Wiley-Liss, Inc.

Key words: β-hairpin; protein engineering; protein stability; protein folding; FGF

INTRODUCTION

Protein architectures are built up from α-helical, β-strand, and turn secondary structure motifs. Among these secondary structures, β-turns are the most common type of nonrepetitive structure recognized in proteins, and comprise about 25% of the residues.[1] Despite this abundance, less is understood regarding the contribution of turns to the structure, stability, and folding of proteins than for α-helices and β-sheets. One reason for this lack of knowledge is that β-turns appear to be far more varied and complex than either α-helices or β-sheets.

Richardson and coworkers[2] have characterized the β-turn as having six distinct types (I, I′, II, II′, VIa, and VIb), as well as a miscellaneous category (IV), based on main-chain ϕ, ψ angles. If a β-turn connects two β-strands that form an antiparallel β-sheet, then it is known as a β-hairpin turn. Thornton and coworkers[3] developed an "X:Y" shorthand for β-hairpin structures whereby X identifies the number of residues required for the turn and Y identifies the hydrogen bonding pattern in the closure of the turn (X equals Y when the closure involves two backbone hydrogen bonds, whereas Y = X + 2 if closure involves one hydrogen bond). Thornton noted that the number of residues in β-hairpin turns typically comprises two to seven residues (X = 2–7), and can be further classified according to different patterns of backbone hydrogen bonding. This complexity makes β-turns a fertile area for biophysical studies of protein stability and folding.

Various reports have characterized the relationship between turn residues and β-hairpin formation using small peptide systems.[4–8] Jimenez and coworkers[9] showed that different turn sequences can alter turn conformation, and consequently, the β-sheet registration of β-hairpins. Conversely, Searle and coworkers[10] reported that turn regions within a protein may be able to maintain their conformation despite variations in their primary structure. Rotondi and Gierasch[8] have shown that two of the seven β-hairpin turns in retinoic acid binding protein I form spontaneously in solution as short peptides, suggest-
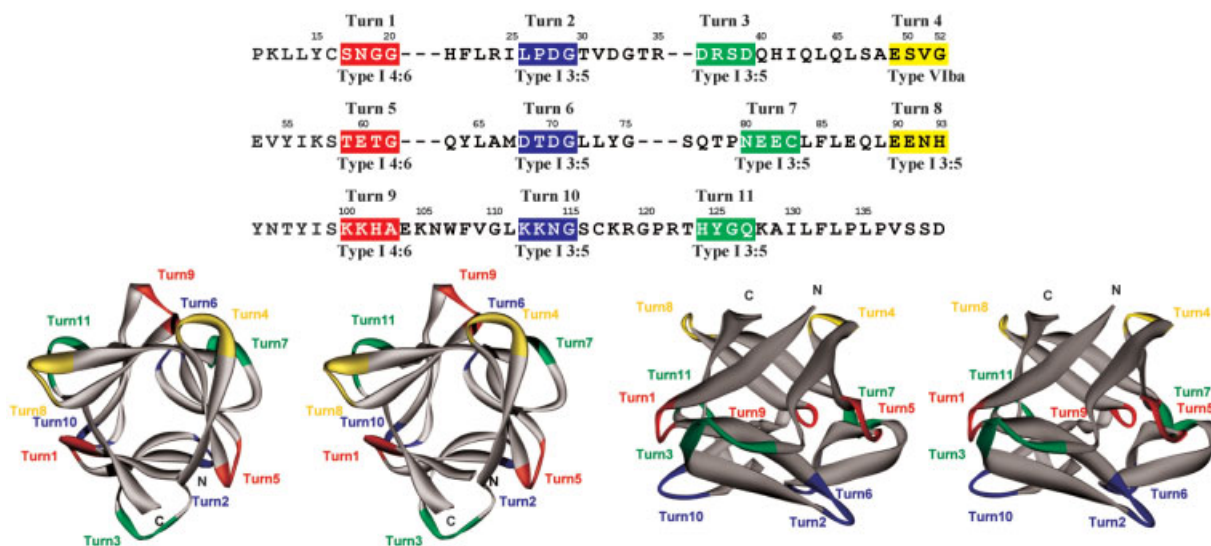
Fig. 1. (Upper panel) The primary structure of FGF-1 aligned to reflect the threefold tertiary structure symmetry inherent in the β-trefoil superfold. The 11 β-turns present in the structure are indicated by the colored text, and the color scheme highlights the symmetric relationship of the turns. The turn type is given below the primary structure. (Lower panel) Relaxed stereodiagram of FGF-1 (PDB accession 1JQZ) viewed down the threefold axis of structural symmetry (left), and a corresponding "side" view (right). The locations of the 11 β-turns are indicated, and colored using the same scheme as in the upper panel. Also shown are the locations of the N- and C-termini.

ing that local sequence may determine some turn structures, while others may be influenced more by the local structural environment. Related to this issue, sequence-swapping mutations in FGF-1, for turn regions that differ in structure, do not result in conformation swapping; suggesting that turn conformation in proteins is influenced more by the local environment than by the turn sequence itself.[11] Thus, turn structure, stability and folding are complicated issues involving interplay between turn sequence and the local structural environment; however, predicable effects of turn mutations upon protein stability and folding are beginning to emerge. In some cases, specific polar interactions between residues i and $i + 2$ in type I 3:5 turns have been implicated in stabilization of the turn structure.[8] In reference to Ala, a Gly residue at the $i + 3$ position in type I 3:5 and 4:6 turns (where the $i + 3$ residue is located in the L-α region of the Ramachandran plot) has been shown in several different proteins to stabilize the structure by 7.3 ± 1.4 kJ/mol.[12] However, much work remains to be done to elucidate the relationship between turn sequence and the local structural environment upon turn structure, stability, and folding.

Human acidic fibroblast growth factor (FGF-1) has a total of 12 β-strands connected by a series of 11 β-turns characteristic of the β-trefoil superfold (Fig. 1). Five of these turns (turns 2, 4, 6, 8, and 10; Fig. 1) are classical β-hairpin turns (β-turns that connect antiparallel β-sheet secondary structure and form a terminal interstrand hydrogen bond). Among these, turns 2, 6, and 10 are related by the threefold structural symmetry of the β-trefoil architecture. Similarly, turns 4 and 8 are related by the threefold structural symmetry (with the N- and C-termini comprising a symmetry-related "discontinuous" turn; Fig. 1). With the exception of turn 4 (which is a type

VIba turn), all of these turns in FGF-1 are type I 3:5 turns. The type I turn is defined by the characteristic main chain angles of the $i + 1$ and $i + 2$ residues within the turn (turn residue $i + 1$ φ ≅ −60°, ψ ≅ −30°; and turn residue $i + 2$ φ ≅ −90°, ψ ≅ 0°), and the 3:5 nomenclature indicates that there are three residues comprising the turn, and the residues that close off the turn do so via a single main chain hydrogen bond.[3] Turns 3, 7, and 11 are also type I 3:5 β-turns (and also related by the threefold structural symmetry), but the connecting secondary structure is not an antiparallel β-sheet (Fig. 1). Turns 1, 5, and 9 are unique in being type I 4:6 β-turns (i.e., containing four instead of three residues within the turn). The β-strands that turns 1 and 5 connect do not primarily hydrogen bond with each other: they diverge almost immediately after the turn, and in each case, contain only a single additional interstrand hydrogen bond before diverging (Fig. 1). Thus, there is some question as to whether β-turns 1 and 5 should be considered as true β-hairpin structures. Turn 9 (symmetry-related to turns 1 and 5) exhibits a structural distortion, due to an apparent three amino acid insertion after the turn (Fig. 1), that eliminates any consideration of it being a β-hairpin type of turn.

This description of the β-turns present in FGF-1 highlights the fact that the predominant turn type is a type I 3:5, but that type I 4:6 turns are present at characteristic symmetry-related positions within the protein architecture. Why are the type I 4:6 turns found exclusively at this particular structural location, and can the FGF-1 architecture be simplified by the utilization of a single turn type (i.e., type I 3:5) at every position where a β-turn is required? To answer this question we have investigated the effects upon the structure, stability, folding, and mitogenic function of FGF-1 mutations designed to convert the type I 4:6 turns into type I 3:5 at both turn 1 and turn 5

locations. The results show that the type I 3:5 turn can potentially be utilized at every location in FGF-1 requiring a β-turn, and produce a stable, foldable polypeptide. The results also suggest that the turn structure in FGF-1 is likely determined by a combination of the length of the turn and the nature of the local turn environment; variations in the turn sequence are unlikely to alter the turn structure, but have an important contribution to the turn stability. Finally, the type I 4:6 turn appears to be important at the turn 1 location in FGF-1 for efficient receptor-binding and mitogenic function.

MATERIALS AND METHODS
Mutagenesis and Expression

All studies utilized a synthetic gene for the 140 amino acid form of human FGF-1[13–16] containing an additional amino-terminal six His tag as previously described.[17] The QuikChange™ site-directed mutagenesis protocol (Stratagene, La Jolla, CA) was used to introduce all point mutations and deletions, and confirmed by nucleic acid sequence analysis (Biomolecular Analysis Synthesis and Sequencing Laboratory, Florida State University). All expression and purification followed previously published procedures.[17] Purified protein was exchanged into 20 mM N-(2-acetamido)iminodiacetic acid (ADA), 100 mM NaCl, 2 mM DTT, pH 6.60 ("ADA buffer") for biophysical studies or 50 mM sodium phosphate, 0.1 M NaCl, 10 mM $(NH_4)_2SO_4$, 2 mM DTT, pH 7.5 ("crystallization buffer") for crystallization.

Crystallization of FGF-1 Mutants

Purified protein in crystallization buffer was concentrated to 9–13 mg/mL and crystals were grown using the hanging-drop vapor diffusion method. Diffraction quality crystals of ΔG19, ΔG19/ΔE60 and S17T/N18T/ΔG19 mutants grew in 1 week at room temperature with 1 mL of reservoir solution containing 2.0–3.5 M sodium formate and 0.9–1.0 M ammonium sulfate in the crystallization buffer. ΔE60 crystals grew within 1 week at room temperature in 10 μL hanging drops by vapor diffusion against 2% of PEG 400, 0.1 M Na-HEPES, 2 M $(NH_4)_2SO_4$.

Data Collection, Molecular Replacement, and Refinement

Diffraction data for ΔG19, ΔE60, and S17T/N18T/ΔG19 mutants were collected using a Rigaku RU-H2R copper rotating anode (λ = 1.54 Å) X-ray generator (Rigaku MSC, The Woodlands, TX) coupled to a Osmic Blue or a Purple confocal mirror system (Osmic, Auburn Hills, MI) and to an R-Axis IIc image plate (Rigaku MSC, The Woodlands, TX) or a MarCCD165 charge-coupled device detector (Mar USA, Evanston, IL). Diffraction data collection for ΔG19/ΔE60 was collected at Southeast Regional Collaborative Access Team (SER-CAT) 22-BM beamline (λ = 1.00 Å) at the Advanced Photon Source, Argonne National Laboratory using a MarCCD225 charge-coupled device detector (Mar USA, Evanston, IL). In each case, crystals were mounted using Hampton Research nylon mounted cryoturns and frozen in a stream of gaseous nitrogen at 100 K.

Diffraction data were indexed, integrated and scaled using the DENZO software package.[18,19] His-tagged wild-type FGF-1 (PDB code: 1JQZ) was used as the search model in molecular replacement of the ΔG19 and ΔE60 mutant structures, and the refined ΔG19 structure was used as the search model in molecular replacement of the ΔG19/ΔE60 and S17T/N18T/ΔG19 mutant structures, using the Crystallography and NMR System software.[20] Model building and visualization utilized the O molecular graphics program.[21]

Isothermal Equilibrium Chemical Denaturation

Protein denaturation was monitored by following the fluorescence signal of the single endogenous Trp residue at position 107, which is ~90% buried in the native structure.[16] Complete details of the instrumentation, data collection, and analysis procedure have been previously reported.[22] Briefly, the fluorescence signal of FGF-1 is atypical in that Trp107 exhibits greater quenching in the native state rather than the denatured state. Excitation at 295 nm provides selective excitation of Trp107 in comparison with the six Tyr residues that are present in the structure.[17,22] Protein samples (10 to 5 μM) in various concentrations of GuHCl/ADA buffer were allowed to equilibrate overnight at room temperature (298 K). Fluorescence scans were collected in triplicate and averaged; buffer traces were collected and subsequently subtracted from the protein scans. All scans were integrated to quantitate the total fluorescence as a function of denaturant concentration. The data was analyzed using a general purpose nonlinear least-squares fitting program (DataFit, Oakdale Engineering, Oakdale, PA) implementing a six parameter, two-state model:[23]

$$F = \frac{F_{0N} + (S_N[D]) + (F_{0D} + (S_D[D]))e^{-((\Delta G_0 + (m[D]))/RT)}}{1 + e^{-((\Delta G_0 + (m[D]))/RT)}} \quad (1)$$

where the denaturant concentration is given by $[D]$, the native state (0 M denaturant) fluorescence intercept and slope are F_{0N} and S_N, respectively, the denatured state fluorescence intercept and slope are F_{0D} and S_D, respectively, and the free energy of unfolding function intercept and slope are ΔG_0 and m, respectively. The ΔG_0 and m-values describe the linear function of the free energy of unfolding as a function of denaturant under isothermal equilibrium conditions (where ΔG_0 is the ΔG value extrapolated to 0 M denaturant, and m-value is reported as $-d\Delta G/d[D]$). The midpoint of the transition, that is, the denaturant concentration where $\Delta G = 0$, is defined as C_m. The effect of a given mutation upon the stability of the protein ($\Delta\Delta G$) was calculated by taking the difference between the C_m values for wild-type and mutant and multiplying by the average of the m values, as described by Pace and Scholtz:[24]

$$\Delta\Delta G = (C_{m\text{wild type}} - C_{m\text{mutant}})(m_{\text{wild type}} + m_{\text{mutant}})/2 \quad (2)$$

where a negative value indicates the mutation is stabilizing in relationship to the wild-type protein.

Unfolding Kinetic Measurements

Native protein samples were dialyzed against ADA buffer overnight at 298 K. Unfolding was initiated by a 1:10 dilution of 25 μM protein into ADA buffer with concentrations of GuHCl varying between 1.5 to 4.5 M. The fluorescence signal associated with protein unfolding was quantified using a Varian Eclipse fluorescence spectrophotometer, with a wavelength of 295 nm for excitation and 350 nm for emission, and maintained at 298 K with a temperature-controlled Peltier cell holder (Varian Inc., Palo Alto, CA). The unfolding kinetics exhibited relaxation times that were appropriate for manual mixing techniques. The data collection strategy was designed to span approximately two to three half-lives, or >80% of the expected fluorescence signal change between the fully native and denatured states.

Folding Kinetic Measurements

Kinetic measurements followed a previously described methodology.[11,12,25,26] Briefly, denatured protein samples were dialyzed overnight against ADA buffer containing 2.5 M GuHCl. Initial studies using manual mixing indicated that the relaxation times for the folding process were more appropriate for stopped-flow data collection. All folding kinetic data was collected using a Kintek SF2000 stopped-flow system (Kintek Corp., Austin, TX). Folding was initiated by a 1:10 dilution of 40 μM denatured protein into ADA buffer with denaturant concentrations varying from 0.25 M GuHCl to the midpoint of denaturation (as determined by the above-described isothermal equilibrium denaturation measurements) in increments of 0.05 M. The data collection strategy was designed to span approximately five half-lives, or >97% of the expected fluorescence signal change between the fully denatured and native states.

Kinetic Analysis

Both folding and unfolding kinetic data was collected in triplicate at each denaturant concentration, with typically six runs per sample and all data being averaged. The kinetic rate constants and amplitudes, as a function of denaturant concentration, were determined from the time-dependent change in fluorescence intensity implementing a single exponential model:

$$I(t) = A\exp(-kt) + C \qquad (3)$$

where $I(t)$ is the intensity of fluorescent signal at time t, A is the corresponding amplitude, k is the observed rate constant for the reaction, and C is a constant corresponding to the asymptotic signal limit. As previously described,[12] FGF-1 exhibits single exponential unfolding behavior throughout the entire range of denaturant concentration; however, folding in low concentrations ($<\sim 0.6$ M) of denaturant exhibits a fast and slow phase. The folding data in the low denaturant concentration regime is therefore fit using a biexponential model:

$$I(t) = A_1\exp(-k_1t) + A_2\exp(-k_2t) + C \qquad (4)$$

Folding and unfolding rate constant data were fit to a global function describing the contribution of both rate constants to the observed kinetics as a function of denaturant ("Chevron" plot) as described by Fersht:[27]

$$\ln(k_{\text{obs}}) = \ln(k_{f0}\exp(m_fD) + k_{u0}\exp(m_uD)) \qquad (5)$$

where k_{f0} and k_{u0} are the folding and unfolding rate constants, respectively, extrapolated to 0 M denaturant, m_f and m_u are the slopes of the linear functions relating $\ln(k_f)$ and $\ln(k_u)$, respectively, to denaturant concentration, and D is denaturant concentration. The fast unfolding rate constant, in the low denaturant regime of folding, is included in the global fit.[12] The change in the ΔG of unfolding ($\Delta\Delta G$) in response to a mutation was determined from the kinetic data using Equation (2) and the following definitions:

$$C_m = \frac{\ln\left(\dfrac{k_{u0}}{k_{f0}}\right)}{m_f - m_u} \qquad (6)$$

$$m-\text{value} = -RT(m_f - m_u) \qquad (7)$$

Cell Proliferation Assay

The mitogenic activity of FGF-1 mutants, as quantified using an NIH 3T3 fibroblast cell proliferation assay, followed previously published procedures.[26] Briefly, NIH 3T3 fibroblasts were initially plated in Dulbecco's modified Eagle's medium (DMEM) (American Type Culture Collection, Manassas, VA) supplemented with 10% (v/v) newborn calf serum (NCS) (Sigma, St. Louis, MO), 100 units of penicillin, 100 μg of streptomycin, 0.25 μg of Fungizone™ and 0.01 mg/mL of gentamicin (Gibco, Carlsbad, CA) ("serum-rich" medium) in T75 tissue culture flasks (Fisher, Pittsburgh, PA). The cultures were incubated at 37°C with 5% CO_2. At 80% cell confluence, the cells were rinsed with 5 mL of cold TBS (0.14 M NaCl, 5.1 mM KCl, 0.7 mM Na_2HPO_4, 24.8 mM Trizma® base, pH 7.4) and subsequently treated with 5 mL of a 0.025% trypsin solution (Invitrogen Corp., Carlsbad, CA). Cell synchronization was initiated by serum starvation in DMEM with 0.5% NCS, 100 units of penicillin, 100 μg of streptomycin, 0.25 μg of Fungizone™ and 0.01 mg/mL of gentamicin ("starvation" medium). The cells were seeded in T25 tissue culture flasks (Fisher, Pittsburgh, PA) at a cell density of 3.0×10^4 cells/cm^2 (representing ~20% confluence). Duplicate flasks were incubated for 48 h at 37°C, the medium supplemented with the appropriate concentration of FGF-1 protein, and incubated for an additional 48 h. After this incubation, the medium was decanted and the cells were washed with 1 mL of cold TBS (pH 7.4). One milliliter of 0.025% trypsin was then added to release the cells from the flask surface, and 2 mL of serum-rich medium were added to dilute and inhibit the trypsin. The cells were counted using a hemacytometer (Hausser Scientific Partnership, Horsham, PA). Experiments were performed in quadruplicate and the cell densities were averaged. The relationship between the cell number and log concentration of added growth factor was fit to a sigmoid function.

TABLE I. Crystallographic Data Collection and Refinement Statistics for FGF-1 Turn Mutants

	$\Delta G19$	$\Delta E60$	$\Delta G19/\Delta E60$	S17T/N18T/$\Delta G19$
		Crystal data		
Space group	P2$_1$	C222$_1$	P2$_1$	C222$_1$
Cell constants (Å)	a=51.4 b=109.2	a=73.2 b=98.0	a=52.5 b=110.9	a=75.9 b=95.1
	c=69.0 β=107.2°	c=109.3	c=68.8 β=103.3°	c=108.2
Resolution (Å)	50–2.10	30–1.89	15–2.60	20–1.85
Mosaicity (°)	0.65	1.31	0.78	0.48
Mol/ASU	4	2	4	2
Matthews coeff. (Å^3/Da)	2.80	2.97	2.90	2.96
		Data collection and processing		
Reflections total	349,160	307,861	225,004	375,859
Reflections unique	41,488	29,814	23,515	33,570
I/σ overall	39.3	28.9	28.6	55.0
I/σ highest shell	5.1	3.1	4.6	7.4
R_{merge} overall (%)	5.7	5.2	7.5	6.7
R_{merge} highest shell (%)	28.4	27.7	31.4	19.9
Completion overall (%)	97.5	93.5	100	99.4
Completion highest shell (%)	80.5	70.5	100	97.1
		Refinement		
Nonhydrogen protein atoms	4518	2254	4482	2274
Solvent molecules/ions	230/7	230/4	90/2	277/15
R_{cryst} (%)	19.8	18.6	19.5	19.6
R_{free} (%)	25.0	22.1	23.5	22.6
RMSD bond length (Å)	0.01	0.01	0.01	0.01
RMSD bond angle (°)	1.4	1.4	1.2	2.0
Ramachandran plot:				
Most favored (%)	91.7	91.2	89.8	91.7
Additional allowed (%)	8.1	8.0	9.3	7.9
Generously allowed (%)	0.2	0.9	0.9	0.4
Disallowed region (%)	0.0	0.0	0.0	0.0

RESULTS

The molecular architecture of FGF-1, a member of the β-trefoil superfold, comprises primarily a β-strand and β-turn secondary structure and essentially no α-helix.[16,28] With two exceptions, the β-hairpin turns in FGF-1 are type I 3:5 ($i + 1$ φ ~−60°, ψ ~−30°, $i + 2$ φ ~−90°, ψ ~0°; three residues separating the first and last residues of the turn, and a single hydrogen bond that closes the turn). The exceptions to this prevalent turn type are turns 1 and 5, which are type I 4:6 β-hairpin turns ($i + 1$ φ ~−60°, ψ ~−30°, $i + 2$ φ ~90°, ψ 0°; four residues separating the first and last residues of the turn, and a single hydrogen bond that closes the turn; note that symmetry-related turn 9 contains a type I 4:6 turn, but is not a defined β-hairpin turn due to an apparent three amino acid insertion that disrupts β-sheet formation[12]). The seemingly atypical type I 4:6 turns in FGF-1 inspired the question of whether a type I 3:5 turn at turns 1 and 5 might somehow be incompatible with stability, folding or function of FGF-1. To answer this question, a single amino acid position within turns 1 and 5 was deleted. Because the type I 4:6 and 3:5 turns differ in the number of residue positions within the turn (with the type I 4:6 turn having an additional residue) we predicted that such a deletion would convert the type I 4:6 turns into 3:5 turns.

A Gly residue at the $i + 3$ position in both type I 3:5 and 4:6 turns has been shown to be critical for overall stability and folding of the turn when the φ, ψ values fall in a characteristic L-α region (0° < φ < +90°, 0° < ψ < +90°) of the Ramachandran plot.[12] The Gly20 and Gly62 residues in the wild type structure are both at the $i + 3$ position within the local type I turn, and are located within the L-α region of the Ramachandran plot; retaining the Gly20 and Gly62 residues therefore appeared essential in the turn mutation design.

X-ray Structures

Diffraction-quality crystals were obtained for the ΔG19, ΔE60, ΔG19/ΔE60, and S17T/N18T/ΔG19 mutant proteins. The ΔE60 and S17T/N18T/ΔG19 mutants crystallized in the same space group (C222$_1$) as wild-type FGF-1 (Table I). The ΔG19 and ΔG19/ΔE60 mutants crystallized in a previously unreported P2$_1$ crystal form. Analysis of this P2$_1$ cell indicated a Matthews' coefficient of ~2.8 Å^3/Da with four molecules in the asymmetric unit. These four molecules were successfully positioned in the ΔG19 cell using the molecular replacement method and wild-type FGF-1 as the search model. This initial solution was subsequently also used as a successful starting model for the refinement of the ΔG19/ΔE60 double mutant.

Gly19 being adjacent to Gly20 in turn 1 of the wild-type protein leads to ambiguity regarding which residue is actually being deleted when constructing a deletion mutation at this position. Analysis of the mutant X-ray structure overlaid onto the wild-type structure shows that the remaining mutant Gly C$^\alpha$ atom is 1.1 Å distal to the C$^\alpha$
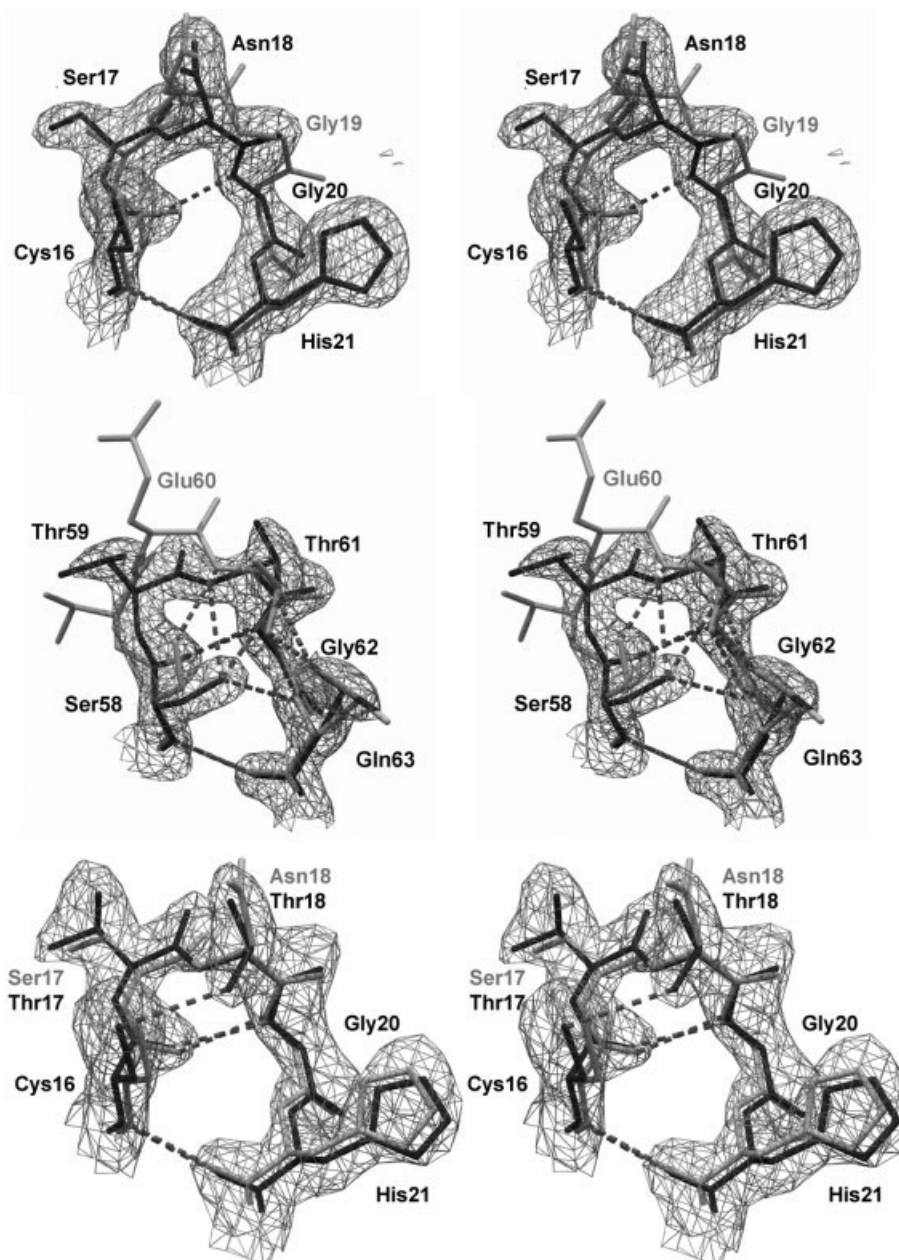
Fig. 2. (Upper panel) Relaxed stereodiagram of an overlay of the turn 1 region in the wild-type FGF-1 structure (light gray) with that of the ΔG19 mutant (dark gray). Also shown is a $2F_o - F_c$ difference electron density map of the ΔG19 mutant contoured at 1.5σ. Turn 1 has converted from type I 4:6 in the wild-type structure to a type I 3:5 in the ΔG19 mutant. (Middle panel) Relaxed stereodiagram of an overlay of the turn 5 region in the wild-type FGF-1 structure (light gray) with that of the ΔE60 mutant (dark gray). Also shown is a $2F_o - F_c$ difference electron density map of the ΔE60 mutant contoured at 1.5σ. Turn 5 has converted from type I 4:6 in the wild-type structure to a type I 3:5 in the ΔE60 mutant. (Lower panel) Relaxed stereodiagram of an overlay of the turn 1 region in the ΔG19 mutant structure (light gray) with that of the S17T/N18T/ΔG19 mutant (dark gray). Also shown is a $2F_o - F_c$ difference electron density map of the S17T/N18T/ΔG19 mutant contoured at 1.5σ. The S17T/N18T mutations in the turn 1 region are accommodated with essentially no change to the turn structure in the ΔG19 mutant background.

atom of Gly20 in the wild-type structure, while it is 2.7 Å distal to the C^α atom of Gly19; thus, the single Gly residue in the mutant structure is most closely associated with the position of Gly20, and therefore, we consider that the Gly deletion mutation represents a deletion of position 19 (i.e., ΔG19).

Analysis of the ΔG19 X-ray structure shows that turn 1 converts from a type I 4:6 to a type I 3:5 turn (Fig. 2). Cys16 and His21 (the residues containing the interstrand hydrogen bond that closes the turn) of the ΔG19 mutant essentially juxtapose with the same residues in the wild-type FGF-1 structure, and the majority of the structural

TABLE II. Thermodynamic Parameters for Turn 1 and Turn 5 FGF-1 Mutant Proteins Determined by Isothermal Equilibrium Denaturation

Protein Mutant	Turn 1 seq	Turn 5 seq	ΔG (kJ/mol)	m-value (kJ/mol M)	C_m (M)	[a]$\Delta\Delta G$ (kJ/mol)
Wild Type	CSNGG	STETG	21.1 ± 0.6	18.9 ± 0.6	1.11 ± 0.01	0.0
Group 1:						
ΔG19	CSNG	*	21.3 ± 0.1	19.1 ± 0.5	1.11 ± 0.02	0.0
ΔT59	*	SETG	14.7 ± 1.2	20.4 ± 1.4	0.72 ± 0.02	7.7
ΔE60	*	STTG	20.7 ± 0.8	22.4 ± 1.2	0.92 ± 0.01	3.9
ΔT61	*	STEG	17.2 ± 0.8	20.3 ± 0.7	0.85 ± 0.01	5.1
ΔG19/ΔE60	CSNG	STTG	19.3 ± 0.7	20.6 ± 0.8	0.94 ± 0.01	3.4
Group 2:						
S17T/N18T/ΔG19	CTTG	*	20.4 ± 0.3	20.6 ± 0.2	0.99 ± 0.01	2.4
S17T/N18T/ΔG19/ΔE60	CTTG	STTG	16.3 ± 0.4	19.8 ± 0.7	0.82 ± 0.01	5.6
C16S/S17T/N18T/ΔG19/ΔE60	STTG	STTG	—	—	—	—
ΔE60/T61D	*	STDG	18.4 ± 1.6	20.4 ± 1.8	0.90 ± 0.02	4.1
T59S/ΔE60/T61N	*	SSNG	16.6 ± 0.4	19.1 ± 0.5	0.87 ± 0.01	4.6
ΔG19/T59S/ΔE60/T61N	CSNG	SSNG	16.00 ± 1.0	17.8 ± 1.2	0.90 ± 0.01	3.9
ΔG19/S58C/T59S/ΔE60/T61N	CSNG	CSNG	13.9 ± 1.6	16.9 ± 1.8	0.82 ± 0.01	5.2

[a]$\Delta\Delta G = (C_{m\text{wild type}} - C_{m\text{mutant}}) * (m_{\text{wild type}} + m_{\text{mutant}})/2$.[24] A negative value for $\Delta\Delta G$ indicates a more stable mutant.
*Indicates wild-type turn sequence for this mutant.

alterations are limited to residue positions Ser17, Asn18, and Gly20 (residues $i + 1$, $i + 2$, and $i + 3$, respectively, in the new turn structure). Asn18 exhibits the greatest structural change, shifting its C^α position by approximately 1.4 Å. The side chain of Asn18 also changes rotamer conformations, from *trans* to *gauche+*; however, the combination of this C^α positional shift and change in side chain rotamer results in the side-chain $N^{\delta2}$ and $O^{\delta1}$ atoms being essentially juxtaposed with the wild-type structure (Fig. 2). This structural juxtaposition maintains a hydrogen bond between the $N^{\delta2}$ atom of Asn18 and the main chain carbonyl group of Leu111 in the local environment (not shown). The side chain of Ser17 also adopts an alternate rotamer conformation in the ΔG19 mutant (from *trans* to *gauche+*), but this side chain in both conformers orients towards solvent and does not appear to participate in any critical hydrogen bonding interactions. Thus, although the ΔG19 mutation converts turn 1 from a type I 4:6 to type I 3:5, key interactions involving the side chains within this turn are essentially maintained, and deletion of Gly19 does not eliminate any substantial interactions associated with this residue.

The X-ray structure of the ΔE60 mutation within turn 5 exhibits both similarities and differences in comparison to the ΔG19 mutation within turn 1. As is the case with the turn 1 ΔG19 structure, the deletion of residue E60 results in the conversion of turn 5 from a type I 4:6 to a type I 3:5 turn, and residue positions Ser58 and Gln63 (the residues containing the inter-strand hydrogen bond that closes the turn) exhibit minimal structural perturbation (Fig. 2). The side chain of Glu60 hydrogen bonds to solvent, and no critical hydrogen bond appears to be disrupted upon its deletion. The C^α of Thr59 shifts by 2.1 Å, the C^α of Thr61 shifts by 0.8 Å, and the C^α of Gly62 shifts by 0.5 Å. Thus, in both turn deletion mutations the adjacent residue on the *amino-terminus* side of the deletion exhibits the largest positional shift. Residue position Ser58 adopts an alter-

nate rotamer conformation, switching from *trans* in the wild-type structure to *gauche−* in the ΔE60 mutant. In forming a type I 3:5 turn, the positional shift of the main chain and side chain of residue Thr61 permits hydrogen bonding of the Thr61 N and $O^{\gamma1}$ atoms with the Ser58 O^γ in the *gauche−* rotamer (Fig. 2). In the wild-type structure Thr59 $O^{\gamma1}$ hydrogen bonds with the main chain carbonyl of position Gln43, whereas, in the ΔE60 mutant, the Thr59 $O^{\gamma1}$ hydrogen bonds with the main chain carbonyl of position Gln40 (not shown). Thus, the turn 5 deletion mutation results in a significantly different hydrogen-bonding arrangement within the turn (whereas, the hydrogen bonding arrangement within the turn 1 deletion mutation is essentially preserved). The structural effects of the ΔG19/ΔE60 double mutant are observed to be essentially the sum of those already described for the ΔG19 and ΔE60 single deletion mutations. Thus, turn 1 and turn 5 appear to be isolated and independent structural environments within the FGF-1 architecture.

The S17T/N18T/ΔG19 mutant exhibits essentially no structural perturbation when compared to the ΔG19 mutant (Fig. 2). The side chain $O^{\gamma1}$ of the introduced Thr18 side chain forms a potential hydrogen bond with the S^γ atom of Cys16. The substitution of Asn18 by Thr eliminates the previously described hydrogen bond between the Asn18 side chain and the main-chain carbonyl of Leu111 in the local environment. These hydrogen bonding changes do not result in any changes to the overall turn type.

Isothermal Equilibrium Chemical Denaturation

The "group 1" mutations in Table II are deletion mutants within the turn 1 or turn 5 regions of FGF-1 that are designed to convert the type I 4:6 turns into type I 3:5 turns. The ΔG19 mutant is accommodated with essentially no detectable effect upon the stability of the protein. In contrast, the individual deletion mutations in turn 5 (Thr59 through Thr61) destabilize the protein 3.9 to 7.7

TABLE III. Folding and Unfolding Kinetic Parameters, and Derived Thermodynamic Parameters, for Turn 1 and Turn 5 FGF-1 Mutant Proteins

Protein Mutant	Turn 1 seq	Turn 5 seq	k_{f0} (s^{-1})	m_f (M^{-1})	k_{u0} ($1\times10^{-3}s^{-1}$)	m_u (M^{-1})	[a]$\Delta\Delta G$ (kJ/mol)
Wild type	CSNGG	STETG	3.75	−6.61	0.81	0.47	—
Group 1:							
$\Delta G19$	CSNG	*	4.99	−6.21	1.66	0.51	0.0
$\Delta T59$	*	SETG	1.78	−7.51	1.71	0.44	5.9
$\Delta E60$	*	STTG	3.32	−7.06	1.26	0.47	2.6
$\Delta T61$	*	STEG	1.92	−7.41	1.00	0.47	4.3
$\Delta G19/\Delta E60$	CSNG	STTG	3.65	−6.14	2.03	0.56	1.2
Group 2:							
S17T/N18T/$\Delta G19$	CTTG	*	3.41	−5.92	2.19	0.80	1.7
S17T/N18T/$\Delta G19/\Delta E60$	CTTG	STTG	2.27	−6.06	3.93	0.80	4.6
C16S/S17T/N18T/$\Delta G19/\Delta E60$	STTG	STTG	—	—	—	—	—
$\Delta E60/T61D$	*	STDG	2.72	−6.91	1.53	0.47	3.2
T59S/$\Delta E60/T61N$	*	SSNG	4.06	−7.77	1.40	0.50	4.3
$\Delta G19/T59S/\Delta E60/T61N$	CSNG	SSNG	3.37	−6.25	2.44	0.56	2.2
$\Delta G19/S58C/T59S/\Delta E60/T61N$	CSNG	CSNG	2.30	−6.51	2.65	0.53	4.0

[a]$\Delta\Delta G = (C_{m\ \text{wild type}} - C_{m\ \text{mutant}})*(m_{\text{wild type}} + m_{\text{mutant}})/2^{24}$ with parameters derived from the folding and unfolding kinetic data. A negative value for $\Delta\Delta G$ indicates a more stable mutant.
*Indicates wild-type turn sequence for this mutant.

kJ/mol, with the least destabilizing mutation being $\Delta E60$. The stability effects of the $\Delta G19/\Delta E60$ combination mutant are essentially additive, and support the independent nature of these two turns as deduced from the X-ray structure data. The "group 2" mutations in Table II are substitution mutations between turns 1 and 5 within the $\Delta G19$ or $\Delta E60$ background proteins (i.e., with type I 3:5 turns at the turn 1 or turn 5 locations). These mutations are designed to probe the effects upon stability when interconverting the turn 1 and turn 5 amino acid sequences. In the first set of mutations within this group, the primary structure of turn 5 is being substituted into turn 1. Combined substitutions at the $i + 1$ and $i + 2$ positions (mutations Ser17Thr and Asn18Thr, respectively) in turn 1 are observed to destabilize the $\Delta G19$ mutant background by 2.4 kJ/mol. Inclusion of the Cys16Ser mutation (at the i position in the turn) renders the protein insoluble (presumably due to the substantial destabilization reported for this point mutation in the wild-type protein)[29]. Similarly, combined substitutions at the $i + 1$ and $i + 2$ positions (mutations Thr59Ser and Thr61Asn, respectively) in turn 5 are observed to destabilize the $\Delta E60$ mutant background by 1.0 kJ/mol. Inclusion of the Ser58Cys mutation (at the i position in the turn) destabilizes the protein an additional 1.4 kJ/mol.

Folding and Unfolding Kinetic Parameters

The mutant folding and unfolding kinetic parameters are listed in Table III. There is generally good agreement between the $\Delta\Delta G$ values derived from the folding and unfolding rate constants and those determined from the isothermal equilibrium denaturation studies (Table II). Thus, the two-state assumption utilized in these analyses appears valid for each mutant. The $\Delta G19$ mutation is associated with an increase in both the rate of folding and unfolding, such that the overall effect upon stability is
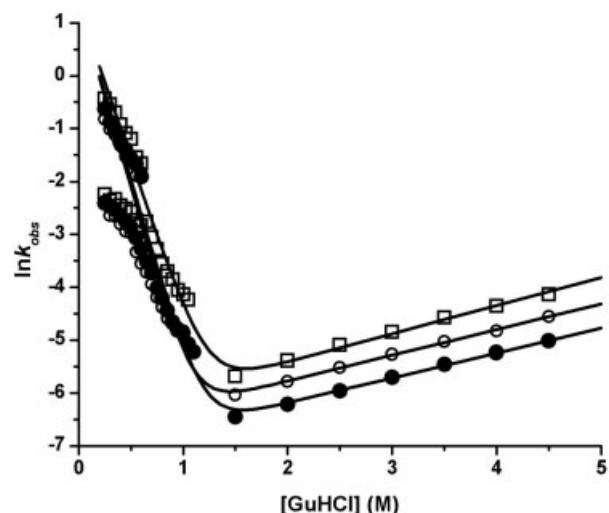

Fig. 3. Folding and unfolding kinetic data "Chevron" plots for wild-type (●), $\Delta G19$ (□), and $\Delta E60$ (○) mutants. The $\Delta G19$ mutant stabilizes the transition state, with minimal effect upon overall stability. The $\Delta E60$ mutant has little effect upon the rate of folding, but increases the rate of unfolding, indicating destabilization of the native state due to structural strain.

minimal; thus, this mutation appears to have stabilized the transition state.[27] The $\Delta E60$ mutation has minimal effect upon the rate of folding, but increases the rate of unfolding, indicating a modest destabilization of the native structure (Fig. 3). Further sequence substitution mutations within the turn 1 and turn 5 regions consistently increase the rate of unfolding, while the effects upon the rate of folding appear variable, but overall, are less significant than the changes observed for the increased rate of unfolding (Table III).
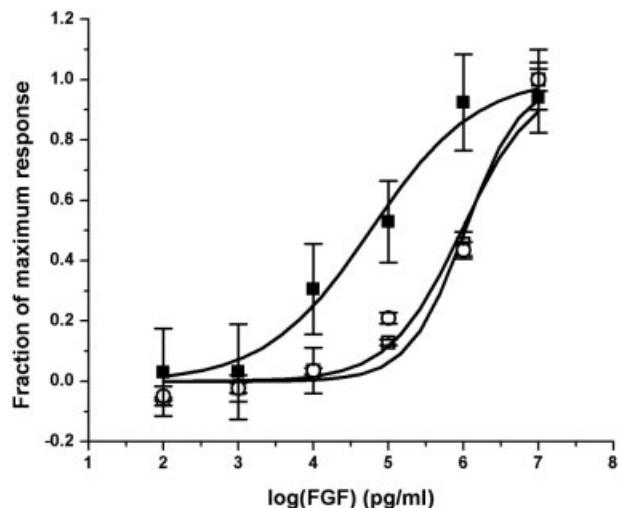
Fig. 4. Mitogenic activity assay of WT and mutant FGF-1 proteins against NIH 3T3 fibroblasts. WT (●), ΔG19 (□), and ΔE60 (○) mutants exhibit EC_{50} values of 60, 1042, and 943 ng/mL, respectively. Standard deviations of the measurements are indicated by the error bars.

Mitogenic Activity

In addition to wild-type FGF-1, mitogenic activity towards NIH 3T3 fibroblasts was determined for the ΔG19 and ΔE60 deletion mutations (Fig. 4). The effective concentration for 50% maximal mitogenic stimulation (EC_{50}) by wild-type FGF-1 was 60 ng/mL; the ΔG19 mutant exhibited an EC_{50} of 1042 ng/mL (~18-fold less mitogenic activity compared to wild-type) and the ΔE60 mutant exhibited an EC_{50} of 943 ng/mL (~16-fold less potent in comparison to the wild-type).

DISCUSSION

Analysis of the ΔG19 mutant structure showed that turn 1 converted from a type I 4:6 to a type I 3:5 β-hairpin turn. Furthermore, the $i + 3$ Gly20 residue in the new turn structure remains located within the L-α region of the Ramachandran plot, thus confirming the importance of retaining this residue. Although we hypothesized that deletion of a residue within the turn would result in formation of a type I 3:5 turn, it seemed likely that there would be an associated stability penalty, possibly severe, given the apparent uniqueness of the type I 4:6 turn at this location in the β-trefoil architecture. Thus, it came as a surprise that the ΔG19 mutant was essentially indistinguishable from the wild-type protein with regard to stability. As previously described in the Results section, the side chains in the new type I 3:5 turn are able to retain essentially equivalent interactions with neighboring groups in comparison to the wild-type structure. Shorter loop lengths are known to be associated with an increase in stability due to reduction in the entropic cost of forming such turns[30] with a consequent increase in the rate of folding.[31,32] Furthermore, the substitution of Gly to non-Gly residues can also stabilize proteins due to the reduction in the entropic gain of unfolding,[33] and a deletion of a Gly residue may therefore similarly stabilize the struc-

ture. Thus, the ΔG19 mutation might be expected to exhibit a favorable entropic effect upon protein stability; however, the observed wild-type equivalent stability suggests that this is being offset by an essentially equivalent enthalpic penalty (i.e., the noncovalent interactions within the turn, and between the turn and surrounding environment, are less optimal than in the wild-type structure).

The folding and unfolding kinetic data shows that the ΔG19 mutant achieves its equivalent stability by concomitant increases in both the folding and unfolding rates (Fig. 3), indicating that this mutation has stabilized the folding transition intermediate. The rate-limiting event in β-hairpin folding in peptide systems has been shown to correspond to formation of the turn (as opposed to formation of the β-sheet secondary structure).[31] Thus, the stabilization of the folding transition state observed for the ΔG19 mutant indicates that formation of the wild-type turn 1 structure contributes to the rate limiting step of FGF-1 folding. The observed stabilization of the folding transition intermediate, combined with the inferred enthalpic penalty for the native structure, suggests that the mutant type I 3:5 turn may self-nucleate more efficiently than the wild-type type I 4:6 turn, but that it is ultimately accommodated less favorably within the native structure. This suggests that there is a need to optimize the enthalpic interactions of the mutant turn with the local environment.

The results indicate that the type I 4:6 turn at turn 1 of FGF-1 can be replaced with a type I 3:5 turn with no significant deleterious effects upon protein stability; however, the NIH 3T3 cell proliferation assay showed an 18-fold reduction in mitogenic activity for the ΔG19 mutant (Fig. 4). Analysis of the available FGF-1/FGFR-2/heparin complex structures shows that turn 1 in FGF-1 interacts with domain D2 of FGFR-2.[34] In particular, the main-chain carbonyl of Ser17 hydrogen bonds with the side-chain N^{ζ} atom of K163 in the receptor. Furthermore, there are extensive van der Waals contacts between K163 of the receptor and the turn 1 region, and these are disrupted upon conversion to the type I 3:5 turn. Thus, although the type I 3:5 turn conformation is compatible with stability and folding of FGF-1, it is deleterious for receptor binding functionality. This suggests that the turn 1 type I 4:6 turn was selected for on the basis of functional considerations.

The X-ray structure data for the ΔE60 mutant shows that the type I 4:6 turn has converted into a type I 3:5 turn (Fig. 2), with Gly62 at the $i + 3$ position and located within the L-α region of the Ramachandran plot. The stability and folding data shows that, unlike ΔG19, a deletion mutation in turn 5 is destabilizing, regardless of position. The best-tolerated deletion mutant within turn 5 is ΔE60, albeit accommodated with a modest 3.9 kJ/mol decrease in stability (Table II). There is essentially no effect upon the rate of folding, but rather an increase in the rate of unfolding (Table III). This suggests that the mutation resulted primarily in destabilization of the native state. The structure of this mutant demonstrates that, unlike the ΔG19 mutant, the hydrogen bonding interactions within
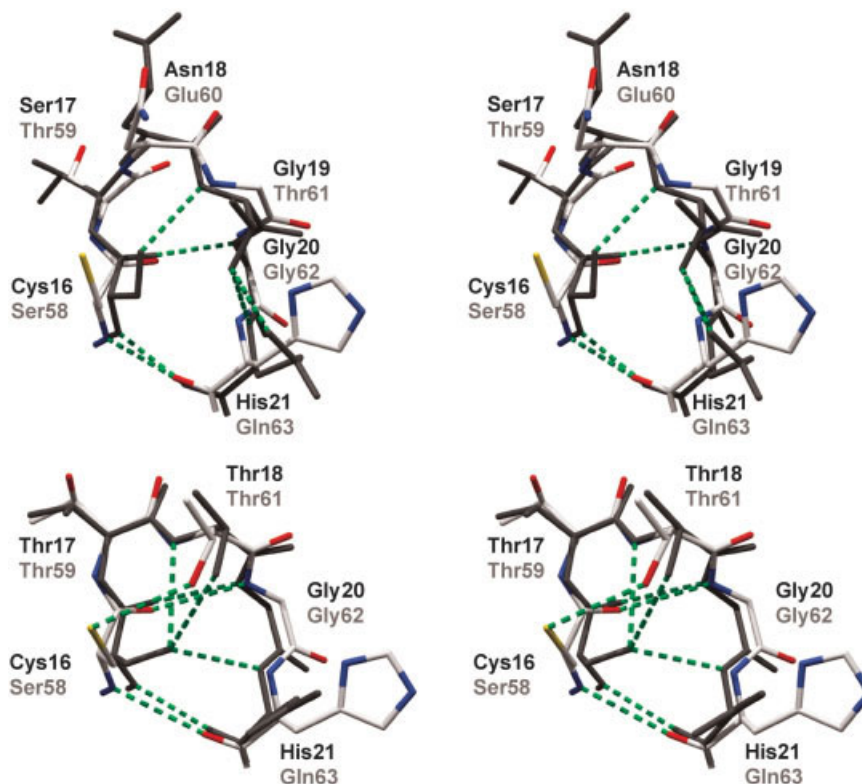
Fig. 5. (Upper panel) Relaxed stereodiagram of an overlay of the turn 1 (CPK color scheme) and turn 5 (gray) regions in wild-type FGF-1 (PDB accession 1JQZ). (Lower panel) Relaxed stereo diagram of an overlay of the turn 1 (CPK color scheme) and turn 5 (gray) regions in the S17T/N18T/ΔG19 and ΔE60 mutants, respectively. The structural similarity of these symmetry-related turns is retained as they are converted from type I 4:6 to type I 3:5 turns.

the turn are substantially altered from the wild-type structure (Fig. 2). Following from the study of Serrano and coworkers,[35] the destabilization is assigned to an increase in strain within the turn, with minimal effects upon overall enthalpy.[35] Thus, we conclude that although the alternative hydrogen-bonding arrangement observed in the ΔE60 mutant may be similar in overall enthalpy to the wild-type turn, it is accomplished with greater structural strain.

The mitogenic activity of the ΔE60 mutant is 16-fold lower than wild-type. Although the ΔE60 mutation is less stable than the ΔG19 mutant, it exhibits slightly greater mitogenic activity. Because turn 5 is not involved in interactions with FGF receptor, we conclude that the reduction in potency of ΔE60 is likely associated with the reduction in stability (and might therefore be recovered by additional mutagenesis designed to increase stability). We attempted to optimize the turn sequence of ΔE60 by replacing the Thr residue at the $i + 2$ position with Asp, because Asp has been reported as the most favorable residue at $i + 2$ position in type I turns.[36] However, this mutation showed no improvement in stability (Table II), suggesting that specific interactions with the local environment are the more critical determinant of turn stability in this case.

β-Hairpin turns 1 and 5 of FGF-1 are related by the threefold tertiary structure symmetry intrinsic to the β-trefoil architecture (Fig. 1). In the wild-type structure these type I 4:6 turns overlay with a root-mean-square deviation of 0.46 Å (for main chain atoms; Fig. 5) despite their amino acid sequence differences. The ΔG19 and ΔE60 deletion mutations convert turns 1 and 5, respectively, to type I 3:5 turns. Again, despite the differences in amino acid sequence, these novel turn structures are essentially identical (Fig. 5), and the main chain atoms of the two turns overlay with a root-mean-square deviation of 0.31 Å. Thus, we hypothesize that the turn structure is dictated by the combined effects of the number of residues within the turn and the fundamental molecular architecture (β-trefoil) that defines the general steric environment of the turn; while the overall stability of the turn is determined by the interactions between the specific residues within the turn (i.e., the amino acid sequence of the turn) and groups comprising the local environment. To test this hypothesis we constructed a series of sequence-swapping mutations between turns 1 and 5 (within the ΔG19 and ΔE60 background forms) (Tables II and III). Such sequence-swapping contributed to additional instability for both turn types, indicating that even in the type I 3:5 turn form, both turn sequences were relatively optimized for their local environment. The X-ray structure of the S17T/N18T/ΔG19 mutant confirmed that sequence-swapping effects were independent of any structural alteration of the basic turn type (Fig. 2).

We have previously reported a study of sequence-swapping mutations for turns 4 and 8 of FGF-1.[11] Although related by the threefold tertiary structure symmetry these turns exhibit different turn types (type VIba for turn 4 and type I 3:5 for turn 8). Sequence-swapping did not alter the overall conformation of these turns, although it did affect overall stability. Thus, the present results are consistent in supporting the hypothesis that basic turn architecture in proteins is largely independent of turn sequence, but that turn sequence influences overall stability. The implication of these observations is that there must be a greater free energy contribution associated with the formation of the secondary and tertiary structures connected by such turns, in comparison to the free energy associated with alternative turn conformations (which might disrupt the connecting structure); this may be most pronounced in β-hairpin turns, where a single amino acid misalignment in a β-strand results in a drastic 180° reorientation of all side chains.

In a related and interesting study by Searle and coworkers,[37] a deletion mutation in β-hairpin turn 1 of ubiquitin (from a type I 3:5 turn to a type I 2:2 turn) resulted in a nonnative register of the associated β-strands in a peptide fragment of ubiquitin.[37] When this deletion mutation was introduced into the intact protein, the nonnative turn structure frustrated the folding of the native state and destabilized the native structure by ~10 kJ/mol. In the present case, the conversion of type I 4:6 to type I 3:5 turns via deletion mutations in FGF-1 is associated with minimal energetic differences between the two turn types. Thus, type I 4:6 and 3:5 turn types may be similar to each other in energetics, but substantially more stable than 2:2 type turns. Furthermore, in cases where β-hairpin turn structures have been shown to interconvert due to sequence changes, the energetic differences between the turn types can be minimal (e.g., turn I′ to II′ conversion in Cro repressor[38]). Thus, different turn structures, even though they may differ in length, can have minimal energetic differences.

Finally, an important implication of the present work for the de novo design of β-trefoil proteins is that a simple type I 3:5 turn might be utilized at every location requiring a β-turn. If designed correctly, in particular, if the turn sequences are chosen so as to favorably interact with atoms comprising the local environment, such a designed protein can be expected to be stable and foldable. The results of the present report thus help to conceptually simplify one important aspect of the architectural design of this fundamental superfold. Of course, if the design principle requires efficient binding to the FGF receptor, then consideration must be made for including a type I 4:6 turn at the turn 1 location, but this is certainly not essential for basic stability or foldability.

ACKNOWLEDGMENTS

REFERENCES

1. Kabsch W, Sander C. Dictionary of protein secondary structure: pattern recognition of hydrogen-bonded and geometrical features. Biopolymers 1983;22:2577–2637.
2. Richardson JS. The anatomy and taxonomy of protein structure. Adv Protein Chem 1981;34:167–339.
3. Sibanda BL, Blundell TL, Thornton JM. Conformation of β-hairpins in protein structures. A systematic classification with applications to modelling by homology, electron density fitting and protein engineering. J Mol Biol 1989;206:759–777.
4. Stanger HE, Gellman SH. Rules for antiparallel beta-sheet design: D-Pro-Gly is superior to L-Asn-Gly for beta-hairpin nucleation. J Am Chem Soc 1998;120:4236–4237.
5. de Alba E, Santoro J, Rico M, Jimenez MA. De novo design of a monomeric three-stranded antiparallel beta-sheet. Protein Sci 1999;8:854–865.
6. Gibbs AC, Bjorndahl TC, Hodges RS, Wishart DS. Probing the determinants of type II′ β-turn formation in peptides and proteins. J Am Chem Soc 2002;124:1203–1209.
7. Blandl T, Cochran AG, Skelton NJ. Turn stability in β-hairpin peptides: investigation of peptides containing 3:5 type I G1 bulge turns. Protein Sci 2003;12:237–247.
8. Rotondi KS, Gierasch LM. Local sequence information in cellular retinoic acid binding protein I: specific residue roles in β-turns. Biopolymers 2003;71:638–651.
9. de Alba E, Rico M, Jimenez MA. The turn sequence directs beta-strand alignment in designed beta-hairpins. Protein Sci 1999;8:2234–2244.
10. Searle MS, Williams DH, Packman LC. A short linear peptide derived from the N-terminal sequence of ubiquitin folds into a water-stable non-native beta-hairpin. Nat Struct Biol 1995;2:999–1006.
11. Kim J, Lee J, Brych SR, Logan TM, Blaber M. Sequence swapping does not result in conformation swapping for the β4/β5 and β8/η 9 β-hairpin turns in human acidic fibroblast growth factor. Protein Sci 2005;14:351–359.
12. Kim J, Brych SR, Lee J, Logan TM, Blaber M. Identification of a key structural element for protein folding within β-hairpin turns. J Mol Biol 2003;328:951–961.
13. Gimenez-Gallego G, Conn G, Hatcher VB, Thomas KA. The complete amino acid sequence of human brain-derived acidic fibroblast growth factor. Biochem Biophys Res Commun 1986;128:611–617.
14. Linemeyer DL, Menke JG, Kelly LJ, Disalvo J, Soderman D, Schaeffer M-T, Ortega S, Gimenez-Gallego G, Thomas KA. Disulfide bonds are neither required, present, nor compatible with full activity of human recombinant acidic fibroblast growth factor. Growth Factors 1990;3:287–298.
15. Ortega S, Schaeffer M-T, Soderman D, DiSalvo J, Linemeyer DL, Gimenez-Gallego G, Thomas KA. Conversion of cysteine to serine residues alters the activity, stability, and heparin dependence of acidic fibroblast growth factor. J Biol Chem 1991;266:5842–5846.
16. Blaber M, DiSalvo J, Thomas KA. X-ray crystal structure of human acidic fibroblast growth factor. Biochemistry 1996;35:2086–2094.
17. Brych SR, Blaber SI, Logan TM, Blaber M. Structure and stability effects of mutations designed to increase the primary sequence symmetry within the core region of a β-trefoil. Protein Sci 2001;10:2587–2599.
18. Otwinowski Z. Oscillation data reduction program. In: Sawyer L, Isaacs N, Bailey S, editors; SERC Daresbury Laboratory, England; 1993. p 56–62.
19. Otwinowski Z, Minor W. Processing of x-ray diffraction data

collected in oscillation mode. Methods Enzymol 1997;276:307–326.

20. Brunger AT, Adams PD, Clore GM, DeLano WL, Gros P, Grosse-Kunstleve RW, Jiang J-S, Kuszewski J, Nilges N, Pannu NS, et al. Crystallography and NMR system (CNS): a new software system for macromolecular structure determination. Acta Crystallogr 1998;D54:905–921.

21. Jones TA, Zou JY, Cowan SW, Kjeldgaard. Improved methods for binding protein models in electron density maps and the location of errors in these models. Acta Crystallogr A 1991;47(Pt 2):110–119.

22. Blaber SI, Culajay JF, Khurana A, Blaber M. Reversible thermal denaturation of human FGF-1 induced by low concentrations of guanidine hydrochloride. Biophys J 1999;77:470–477.

23. Eftink MR. The use of fluorescence methods to monitor unfolding transitions in proteins. Biophys J 1994;66:482–501.

24. Pace CN, Scholtz JM. Measuring the conformational stability of a protein. In: Creighton TE, editor. Protein structure: a practical approach. Oxford: Oxford University Press; 1997. p 299–321.

25. Brych SR, Kim J, Logan TM, Blaber M. Accommodation of a highly symmetric core within a symmetric protein superfold. Protein Sci 2003;12:2704–2718.

26. Brych SR, Dubey VK, Bienkiewicz E, Lee J, Logan TM, Blaber M. Symmetric primary and tertiary structure mutations within a symmetric superfold: a solution, and not a constraint, to achieve a foldable polypeptide. J Mol Biol 2004;344:769–780.

27. Fersht AR. Kinetics of protein folding. New York: W.H. Freeman and Co.; 1999.

28. Murzin AG, Lesk AM, Chothia C. β-Trefoil fold. Patterns of structure and sequence in the kunitz inhibitors interleukins-1β and 1α and fibroblast growth factors. J Mol Biol 1992;223:531–543.

29. Culajay JF, Blaber SI, Khurana A, Blaber M. Thermodynamic characterization of mutants of human fibroblast growth factor 1 with an increased physiological half-life. Biochemistry 2000;39:7153–7158.

30. Nagi AD, Regan L. An inverse correlation between loop length and stability in a four-helix-bundle protein. Fold Des 1997;2:67–75.

31. Du D, Zhu Y, Huang CY, Gai F. Understanding the key factors that control the rate of beta-hairpin folding. Proc Natl Acad Sci USA 2004;101:15915–15920.

32. Dyer RB, Maness SJ, Peterson ES, Franzen S, Fesinmeyer RM, Andersen NH. The mechanism of beta-hairpin formation. Biochemistry 2004;43:11560–11566.

33. Matthews B, Nicholson H, Becktel W. Enhanced protein thermo-stability from site-directed mutations that decrease the entropy of unfolding. Proc Natl Acad Sci USA 1987;84:6663–6667.

34. Pellegrini L, Burke DF, von Delft F, Mulloy B, Blundell TL. Crystal structure of fibroblast growth factor receptor ectodomain bound to ligand and heparin. Nature 2000;407:1029–1034.

35. Ventura S, Vega MC, Lacroix E, Angrand I, Spagnolo L, Serrano L. Conformational strain in the hydrophobic core and its implications for protein folding and design. Nat Struct Biol 2002;9:485–493.

36. Hutchinson EG, Thornton JM. A revised set of potentials for beta-turn formation in proteins. Protein Sci 1994;3:2207–2216.

37. Platt GW, Simpson SA, Layfield R, Searle MS. Stability and folding kinetics of a ubiquitin mutant with a strong propensity for nonnative beta-hairpin conformation in the unfolded state. Biochemistry 2003;42:13762–13771.

38. Mollah AK, Stennis RL, Mossing MC. Stability of monomeric Cro variants: isoenergetic transformation of a type I′ to a type II′ beta-hairpin by single amino acid replacements. Protein Sci 2003;12:1126–1130.